ORIGINAL ARTICLE

The Metabolic Epicenter of Supratentorial Gliomas: A ^{1}H-MRSI Study

Tejas Sankar, Yevgeniy E. Kuznetsov, Robert W. Ryan, Zografos Caramanos, Samson B. Antel, Douglas L. Arnold, Mark C. Preul

ABSTRACT: ***Background:*** Assessing the impact of glioma location on prognosis remains elusive. We approached the problem using multivoxel proton magnetic resonance spectroscopic imaging (^{1}H-MRSI) to define a tumor "metabolic epicenter", and examined the relationship of metabolic epicenter location to survival and histopathological grade. ***Methods:*** We studied 54 consecutive patients with a supratentorial glioma (astrocytoma or oligodendroglioma, WHO grades II-IV). The metabolic epicenter in each tumor was defined as the ^{1}H-MRSI voxel containing maximum intra-tumoral choline on preoperative imaging. Tumor location was considered the X-Y-Z coordinate position, in a standardized stereotactic space, of the metabolic epicenter. Correlation between epicenter location and survival or grade was assessed. ***Results:*** Metabolic epicenter location correlated significantly with patient survival for all tumors ($r^2 = 0.30$, $p = 0.0002$) and astrocytomas alone ($r^2 = 0.32$, $p = 0.005$). A predictive model based on both metabolic epicenter location and histopathological grade accounted for 70% of the variability in survival, substantially improving on histology alone to predict survival. Location also correlated significantly with grade ($r^2 = 0.25$, $p = 0.001$): higher grade tumors had a metabolic epicenter closer to the midpoint of the brain. ***Conclusions:*** The concept of the metabolic epicenter eliminates several problems related to existing methods of classifying glioma location. The location of the metabolic epicenter is strongly correlated with overall survival and histopathological grade, suggesting that it reflects biological factors underlying glioma growth and malignant dedifferentiation. These findings may be clinically relevant to predicting patterns of local glioma recurrence, and in planning resective surgery or radiotherapy.

RÉSUMÉ: Épicentre métabolique des gliomes sustentoriels : une étude SRM 1H. ***Contexte :*** L'impact de la localisation d'un gliome sur le pronostic demeure difficile à déterminer. Nous avons abordé ce problème au moyen de l'imagerie par spectroscopie « multivoxel » par résonance magnétique de proton (SRM 1H) afin d'identifier l' « épicentre métabolique » de la tumeur et d'examiner la relation entre la localisation de l'épicentre métabolique d'une part et la survie et le grade anatomopathologique d'autre part. ***Méthodes :*** Nous avons étudié 54 patients consécutifs porteurs d'un gliome sustentoriel (astrocytome ou oligodendrogliome, grades II à IV selon la classification de l'OMS). L'épicentre métabolique de chaque tumeur a été défini comme étant le voxel SRM 1H contenant le maximum de choline intratumorale à l'imagerie préopératoire. La localisation de la tumeur était déterminée par la position des coordonnées X-Y-Z, dans un espace stéréotaxique standardisé, de l'épicentre métabolique.Nous avons évalué la corrélation entre le siège de l'épicentre et la survie ou le grade de la tumeur. ***Résultats :*** Le siège de l'épicentre métabolique avait une corrélation significative avec la survie des patients quelle que soit la tumeur ($r2 = 0,32$; $p = 0,005$) ainsi que si l'astrocytome était considéré seul. Un modèle prévisionnel basé sur le siège de l'épicentre de la tumeur et son grade anatomopathologique expliquait 70% de la variabilité du temps de survie, ce qui améliore beaucoup la prédiction de la survie basée seulement sur l'anatomopathologie. Le siège de l'épicentre avait également une corrélation significative avec le grade ($r2 = 0,25$; $p = 0,001$) : l'épicentre métabolique des tumeurs de haut grade était plus près du point cérébral médian. ***Conclusions :*** Le concept de l'épicentre métabolique élimine plusieurs problèmes reliés aux méthodes actuelles de classification du siège d'un gliome. Le siège de l'épicentre métabolique est fortement corrélé à la survie globale et au grade anatomopathologique, ce qui suggère qu'il soit le reflet de facteurs biologiques sous-jacents à la croissance du gliome et à sa dédifférenciation maligne. Ces observations pourraient être pertinentes au point de vue clinique pour prédire les profils de récidives locales des gliomes et pour planifier la chirurgie ou la radiothérapie.

Can. J. Neurol. Sci. 2009; 36: 696-706

Supratentorial gliomas are the most frequently diagnosed primary brain tumors in adults.[1] Despite representing only 1.5% of all malignancies,[2] they are a significant cause of cancer-related death in the general population.[3] As a result, a considerable body of research has focused on identifying prognostic markers for patients with these tumors. Although no list of such markers is universally accepted, many authors consistently agree that histopathological grade,[4-7] patient age,[8-12]

From the Neurosurgery Research Laboratory (TS, RWR, MCP), Division of Neurological Surgery, Barrow Neurological Institute, St. Joseph's Hospital and Medical Center, Phoenix, Arizona, USA; MR Spectroscopy Unit (YEK, ZC, SBA, DLA), McConnell Brain Imaging Centre, Departments of Neurology and Neurosurgery, McGill University, Montreal Neurological Institute, Montreal, Quebec, Canada.

Received June 9, 2008. Final Revisions Submitted June 10, 2009.

Correspondence to: Mark C. Preul, Division of Neurological Surgery, Barrow Neurological Institute, St. Joseph's Hospital and Medical Center, 350 W. Thomas Road, Phoenix, Arizona, 85013, USA. Email: neuropub@chw.edu.

and Karnofsky Performance Status (KPS)[1] are among the most important predictors of response to therapy and outcome.

Previous studies have attempted to examine the impact of the location of supratentorial gliomas on prognosis, but have come to conflicting conclusions because a universally accepted method for classifying glioma location is lacking.[13] Most frequently, gliomas have been grouped according to the cerebral lobes (frontal, parietal, temporal, or occipital) that they occupy. Such an approach is flawed because tumors crossing lobar boundaries and occupying portions of more than one lobe may be misclassified. The approach is doubly inaccurate because it fails to account for the considerable regional heterogeneity in growth characteristics and aggressive potential often observed within a given glioma.[14] Consequently, defining glioma location in a biologically relevant manner, using a precise and quantitative classification system, might increase its prognostic significance while potentially furthering our overall understanding of how gliomas grow and spread.

Proton magnetic resonance spectroscopy (^{1}H-MRS) is a noninvasive means of assessing metabolite concentrations in brain tumor tissue *in vivo*. Single voxel ^{1}H-MRS, which can determine the metabolite profile across a single large region of a tumor, improves on the diagnostic specificity of conventional magnetic resonance imaging (MRI) for supratentorial glioma.[15-18] Since the early 1990s, multivoxel ^{1}H-MRS imaging, which elucidates metabolite concentrations within small individual volume units (voxels) within a tumor, has allowed regional metabolic variations within gliomas to be assessed. Intratumoral variations in choline (Cho) have been of particular interest. Cho is a metabolic marker of cell membrane turnover and cellular proliferation,[18-24] and a higher total Cho concentration within a glioma may be associated with increasing grade.[25-27] Early work using ^{1}H-MRSI suggested that the "hottest" Cho region within a tumor may represent the site of highest tumor malignancy.[27] This suggestion has since been supported by studies reporting that cellular proliferative activity within biopsy specimens, as measured by the Ki-67 labeling index, is correlated with Cho concentration in ^{1}H-MRSI voxels corresponding to biopsy location.[23,25,28,29]

Presumably, gliomas which appear to arise from the same part of the brain may actually have very different patterns of intratumoral proliferative activity as represented by their intratumoral distribution of Cho. These different patterns of intratumoral metabolism may in turn produce different clinical courses and portend different prognoses. Consequently, we decided to define the location of a glioma as the location of its point of maximum proliferative activity, represented by the ^{1}H-MRSI voxel containing maximum intratumoral concentration of Cho. We called this voxel the "metabolic epicenter", and defined its location as its X-Y-Z coordinate position in a standardized stereotactic coordinate space.

Based on this novel definition, the objectives of this study were as follows: (1) to determine whether the location of the metabolic epicenter of a supratentorial glioma is related to survival; and, (2) to determine if a relationship exists between the location of the metabolic epicenter of a supratentorial glioma and its histopathological grade.

Materials and Methods

Subjects

We examined the hospital and clinic charts of 60 consecutive patients starting in May 1999 who were diagnosed as having a supratentorial glioma and who were included in the ^{1}H-MRSI brain tumor database at the Montreal Neurological Institute and Hospital (MNI). Patients were included in the study only if they had been closely followed in our brain tumor clinic, if their survival information was available (i.e., either exact length of survival or right-censored survival data), and if they had undergone complete ^{1}H-MRSI examinations.

Patients whose eventual outcome was determined largely by complications unrelated to tumor growth rather than by tumor progression alone were excluded. Therefore, three patients who died of intracranial or somatic postoperative complications within 30 days of surgery were excluded. One patient with clearly multifocal glioma was excluded because tumors in all other patients were unifocal. Two patients who died on unknown dates and did not survive for at least 12 months (i.e., left-censored) were also excluded because the estimate of their length of survival was judged exceedingly imprecise.

The median age of the remaining 54 patients who were included in the study (Table 1) was 44 years (range 19 to 81.4 years). In 51 of these cases, tumors were histologically assessed by a neuropathologist based on tissue samples obtained via an open debulking procedure (n = 30) or via stereotactic biopsy (n = 21). The remaining three patients did not undergo tumor biopsy because their general medical condition was poor. In each of these three cases, however, glioblastoma multiforme (GBM) was confirmed on postmortem neuropathological examination. All study patients were treated according to conventional treatment protocols (e.g., surgical debulking, radiation, and chemotherapy) as deemed appropriate for their histopathologic diagnosis and clinical status.

^{1}H-MRSI Acquisition

Each patient underwent pretreatment conventional MRI and ^{1}H-MRSI scanning. The patients were deemed eligible for ^{1}H-MRSI because they each had a brain tumor that was considered supratentorial on conventional MRI and was sufficiently large for the ^{1}H-MRSI study (i.e., at least 1.5 cm in the craniocaudal dimension). Conventional MRIs and two-dimensional multi-voxel ^{1}H-MRSI scans were acquired using a 1.5 Tesla unit (Gyroscan ACS II/III Philips Medical Systems, Best, The Netherlands).

For ^{1}H-MRSI, a large region of interest (ROI) was defined for selective excitation using standard spin-echo proton density-weighted images (TR/TE = 2100/30 , 250 x 250 mm^2 field of view (FOV), 204 x 256 matrix) in three planes. These ROIs included the entire tumor as well as contralateral or remote normal-appearing brain tissue. The ROIs were aligned parallel to transverse MRI slices and ranged from 70 to 120 mm anteroposteriorly, from 75 to 120 mm mediolaterally, and from 14 to 24 mm craniocaudally. We used a volume-selected method of ^{1}H-MRSI to acquire spectroscopic data tomographically in 8 mm slices within the ROI; we could not use true three-dimensional multivoxel MRSI since this technology was

https://doi.org/10.1017/S0317167100008301 Published online by Cambridge University Press

Table 1: Patient age, survival, histopathological diagnosis, grade, and metabolic epicenter coordinates

Case	Age (years)	Survival (months)	Tumor Type	Tumor Grade (WHO II-IV)	Max Cho X[b]	Max Cho Y[b]	Max Cho Z[b]
1	34.3	0.2	Astrocytoma	IV	0.16	0.05	12
2	55.9	0.6	Oligodendroglioma	II	0.42	0.16	28
3	34.2	0.8	Astrocytoma	IV	0.07	0.15	7
4	48.4	1.1	Astrocytoma	IV	0.03	0.29	19
5	57.4	1.3	Astrocytoma	IV	0.26	0.27	22
6	42.5	1.5	Astrocytoma	IV	0.04	0.13	12
7	68.8	1.6	Astrocytoma	IV	0.37	0.05	41
8	62.1	2.1	Astrocytoma	IV	0.08	0.22	11
9	44.6	2.3	Astrocytoma	IV	0.07	0.17	7
10	81.4	2.4	Astrocytoma	IV	0.19	0.15	15
11	64.5	2.6	Astrocytoma	IV	0.10	0.01	0
12	73.2	2.7	Astrocytoma	IV	0.15	0.00	15
13	60.4	3.0	Astrocytoma	IV	0.30	0.07	19
14	65.0	4.0	Astrocytoma	IV	0.37	0.06	12.7
15	46.1	4.5	Astrocytoma	IV	0.06	0.35	24
16	29.6	4.6	Astrocytoma	IV	0.12	0.20	24
17	41.6	5.2	Oligodendroglioma	III	0.15	0.23	20
18	38.3	6.3	Astrocytoma	IV	0.06	0.07	20
19	58.5	8.4	Astrocytoma	III	0.03	0.10	31
20	29.1	8.7	Astrocytoma	IV	0.00	0.08	11
21	45.5	11.7	Astrocytoma	III	0.29	0.27	30
22	43.9	12.8	Astrocytoma	IV	0.13	0.26	5
23	52.4	15.4	Astrocytoma	IV	0.00	0.26	22
24	43.8	15.8	Astrocytoma	IV	0.19	0.00	33
25	33.4	22.2	Astrocytoma	III	0.02	0.25	23
26	25.0	23.0	Oligodendroglioma	III	0.27	0.03	15
27	42.0	23.4	Astrocytoma	IV	0.07	0.12	24
28	44.0	30.2	Oligodendroglioma	II	0.11	0.21	37
29	35.8	32.4	Astrocytoma	III	0.21	0.06	15
30	22.5	38.0	Oligodendroglioma	III	0.16	0.24	28
31	39.6	50.5[a]	Astrocytoma	II	0.13	0.23	48
32	25.2	52.4[a]	Oligodendroglioma	II	0.30	0.09	46
33	29.4	53.9[a]	Astrocytoma	II	0.30	0.10	16
34	46.3	55.5[a]	Oligodendroglioma	II	0.07	0.05	4
35	49.2	58.0	Oligodendroglioma	III	0.32	0.01	7.5
36	32.3	62.6[a]	Oligodendroglioma	II	0.18	0.14	44
37	49.4	64.1[a]	Astrocytoma	II	0.28	0.14	1
38	49.5	66.4[a]	Oligodendroglioma	II	0.16	0.18	38
39	54.0	68.7[a]	Oligodendroglioma	III	0.09	0.24	46
40	27.5	70.1[a]	Astrocytoma	II	0.28	0.09	15
41	58.1	71.0	Astrocytoma	II	0.28	0.04	45
42	41.6	72.2	Oligodendroglioma	II	0.33	0.12	34
43	45.9	72.3[a]	Oligodendroglioma	II	0.21	0.29	60
44	37.9	95.1[a]	Astrocytoma	III	0.30	0.03	15
45	46.6	96.6[a]	Oligodendroglioma	III	0.23	0.15	14
46	28.8	96.9[a]	Astrocytoma	III	0.10	0.04	54
47	26.1	98.4[a]	Oligodendroglioma	II	0.22	0.18	38
48	53.2	98.5[a]	Astrocytoma	II	0.43	0.07	15
49	19.0	101.9[a]	Astrocytoma	III	0.36	0.27	11
50	56.7	102.0[a]	Oligodendroglioma	III	0.12	0.26	42
51	50.0	103.5[a]	Astrocytoma	II	0.24	0.08	9
52	34.2	105.6[a]	Astrocytoma	II	0.03	0.10	44
53	22.2	108.7[a]	Astrocytoma	II	0.25	0.25	20
54	37.8	110.9[a]	Oligodendroglioma	II	0.30	0.08	6

[a] right-censored case surviving beyond end of study, [b] Max Cho X, Max Cho Y, Max Cho Z = raw coordinates of voxel identified as metabolic epicenter

https://doi.org/10.1017/S0317167100008301 Published online by Cambridge University Press

unavailable when the study began. While we did not use an outer-volume lipid-suppression sequence, unwanted lipid signal was avoided by making sure that the edges of the ROIs did not extend into the skull. ^{1}H-MRSI scans were always obtained before intravenous contrast was administered. In every case, the ROI was determined by the senior author (MCP).

Spectra were obtained using a 90º-180º-180º (i.e., PRESS) pulse sequence for volume selection. Water was suppressed by selective excitation. The following acquisition parameters were used: an interpulse delay (TR) of 2000 ms, a spin-echo refocusing time (TE) of 272 ms, a FOV of 250 x 250 mm^2, 32 x 32 phase encoding steps, and 1 signal average per phase-encoding step. The water-suppressed ^{1}H-MRSI image was followed by a nonwater-suppressed image obtained using a TR of 850 ms, a TE of 272 ms, a FOV of 250 x 250 mm^2, and 16 x 16 phase encoding steps. To correct for artifact arising from inhomogeneities in the magnetic field, the water-suppressed ^{1}H-MRSI was divided by the unsuppressed ^{1}H-MRSI after zero-filling the latter to 32 x 32 profiles. This correction yielded a nominal voxel (i.e., tissue volume) size of 0.7ml. Total imaging time, including ROI definition, shimming, gradient tuning, and ^{1}H-MRSI acquisition, ranged from 55 min to 85 minutes.

^{1}H-MRSI Postprocessing

The ^{1}H-MRSI data were post-processed with in-house software (AVIS, Samson Antel, MRS Unit, Montreal Neurological Institute and Hospital, Montreal, Quebec, Canada). The spectral bandwidth was 2000 Hz with 1024 digitized complex points. Resonance intensity measurements (expressed in volts per hertz) were obtained in each voxel for five of the major resonances observed in the T2-weighted ^{1}H-MRSI spectrum of brain tumors *in vivo*. Expressed as the difference in parts per million (ppm) between the resonant frequency of the compound of interest and that of tetramethylsilane, these five resonances included Cho at 3.2 ppm, creatine at 3.0 ppm, N-acetyl aspartate at 2.0 ppm, lactate at 1.3 ppm, and lipid at 0.9 ppm. Metabolite resonance intensities were determined by the area of Gaussian line-shapes, which were fitted to the resonance peaks relative to a baseline computed from a moving average of the noise regions of each spectrum. Only voxels fully within the tumor mass as outlined on conventional T2-weighted MRI were considered for inclusion in the study. Presumed areas of cyst or necrosis were excluded. In each case the voxel containing maximum intratumoral Cho (max Cho) was identified - this was the metabolic epicenter.

Definition of a Standardized Coordinate System

We used a three-dimensional Cartesian system to describe the location of the metabolic epicenter using X, Y, and Z coordinates. The X coordinate described the mediolateral position, the Y coordinate described the anteroposterior position, and the Z coordinate described the craniocaudal position. The intersection of the X, Y, and Z axes represented the geometric midpoint of the brain and was called the cerebral zero point.

Because of variations in head position and brain shape among patients, the coordinates of the metabolic epicenter in each patient were determined as follows. First, an in-house feature-matching algorithm was used to match the axial ^{1}H-MRSI slice containing the metabolic epicenter anatomically to a corresponding slice generated by a validated MRI simulator developed at the Montreal Neurological Institute.[30] The position assigned to this slice by the simulator became the Z coordinate (Figure1A). In our system, the Z coordinate of the metabolic epicenter was the distance, measured in number of axial slices,

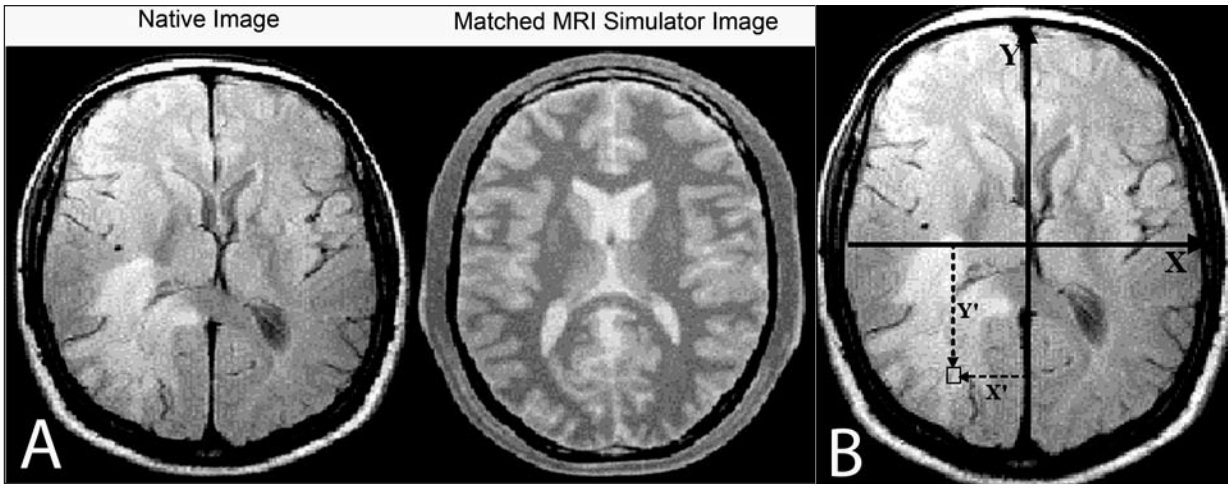

Figure 1: *(A) Determination of the Z coordinate of tumor metabolic epicenter. For each patient, the axial slice containing the max Cho voxel was anatomically matched with an image generated by a stereotactic MRI simulator. The Z coordinate of the corresponding matched image was then assumed to be the Z coordinate of the metabolic epicenter. (B) Determination of the X and Y coordinates of tumor metabolic epicenter. On the axial slice containing the max Cho voxel, the Y axis (Y) was defined at the cerebral midline, and the X axis (X) was defined perpendicular to the Y axis. The open box represents the position of the metabolic epicenter. X' and Y' are the projections of the metabolic epicenter onto the X and Y axes, respectively. X and Y coordinates were determined by dividing each projection by the total length of the corresponding axis.*

https://doi.org/10.1017/S0317167100008301 Published online by Cambridge University Press

between the craniocaudal midpoint of a theoretical "average" brain and the slice containing the max Cho voxel.

On this same slice, the Y axis was set along the cerebral midline, and the X axis was set perpendicular to the Y axis. X and Y coordinates for the metabolic epicenter were then determined by dividing the projection of the metabolic epicenter onto the X and Y axes by the length of each respective axis (Figure 1B). No direction was chosen as negative along any axis, since we were interested in assessing variations in the absolute distance of the metabolic epicenter from the zero point.

Statistical Analysis

Cox proportional hazards regression analysis was performed to generate a model correlating survival with the X, Y, and Z coordinates of the metabolic epicenter. The amount of variability (r^2) in the dependent variable (i.e., survival) accounted for by the independent variable (i.e., metabolic epicenter location) was determined, and the goodness-of-fit of the model was evaluated by performing Chi-squared (χ^2) analysis. To determine whether metabolic epicenter location carried any prognostically significant information independent of histopathological grade, tumor grade was added as a feature in a second model. Feature significance and goodness-of-fit were then recomputed. Astrocytomas and oligodendrogliomas, while sharing some common glial lineage, nonetheless behave much differently in most clinical situations, with astrocytomas tending to behave more aggressively for a given WHO grade. For this reason, we also repeated our analyses on the subgroup of astrocytomas alone. We controlled for age and KPS at diagnosis in all models.

The absolute distance of the metabolic epicenter from the zero point was computed for each patient using the formula: distance = $SQRT(X^2 + Y^2 + Z^2)$, where X, Y, and Z were the

Table 2: Results of Cox proportional hazards regression modeling: significance and regression coefficients of features predictive of survival

Model	Feature[a]	χ^2 [b]	df[c]	B [SE][d]	p-value*
Max Cho Location only, all tumors	Complete model [$\mathbf{r^2=0.3}$]	19.6	3		0.0002
	Z coordinate	14.9	1	-0.096 [0.026]	0.0001
	X coordinate	15	1	-11.4 [3]	0.0001
	X*Z	8.6	1	0.38 [0.13]	0.003
Max Cho Location and Grade, all tumors	Complete model [$\mathbf{r^2=0.7}$]	57	5		<0.0001
	Grade	37.5	2	II: -3.8 [0.7] III: -2 [0.6]	<0.0001
	Z coordinate	8.4	1	-0.1 [0.03]	0.0004
	X coordinate	5	1	-8.6 [4]	0.02
	X*Z	8.5	1	0.5 [0.2]	0.004
Grade only, all tumors	Complete model [$\mathbf{r^2=0.58}$]	47.4	2		<0.0001
	Grade	47.4	2	II: -3.6 [0.7] III: -2.3 [0.5]	<0.0001
Max Cho Location only, astrocytoma subgroup	Complete model [$\mathbf{r^2=0.32}$]	6.3	3		0.017
Max Cho Location and Grade, astrocytoma subgroup	Complete model [$\mathbf{r^2=0.72}$]	26.8	5		<0.0001
	Grade	17.8	2	II: -3.4 [0.8] III: -1.7[0.7]	<0.0001

[a]Feature = individual factors contained in the regression model used to predict survival. Strength of correlation is indicated by r^2; [b]χ^2 = Chi-squared ratio; [c]df = degrees of freedom; [d]B = regression coefficient; SE = standard error
*only features attaining statistical significance at a level of $p < 0.05$ are included here

https://doi.org/10.1017/S0317167100008301 Published online by Cambridge University Press

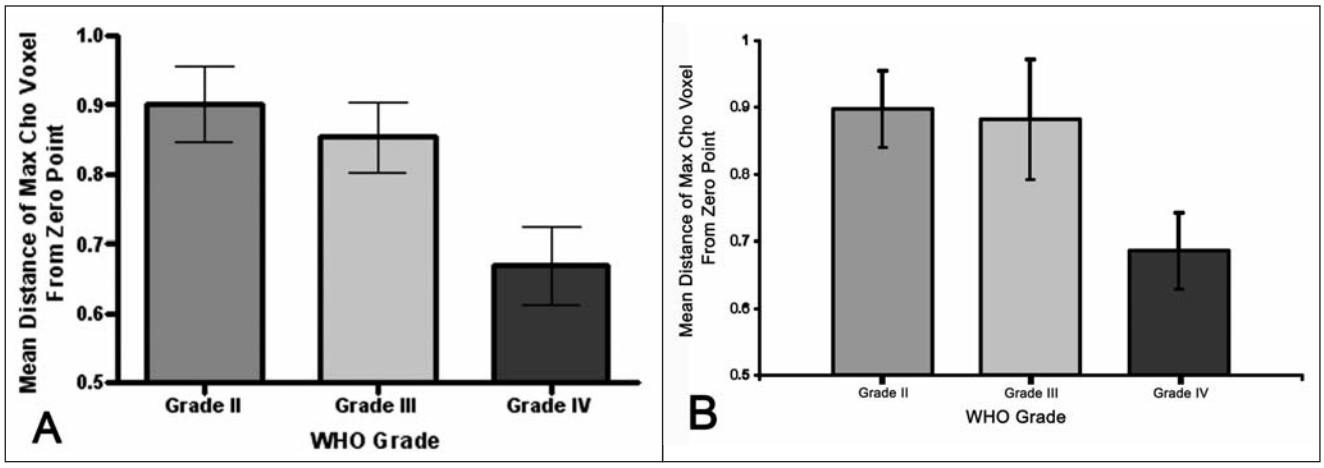

Figure 2: *(A) Metabolic epicenter location versus tumor histopathological grade for all tumor types. On average, grade IV tumors had a significantly deeper metabolic epicenter location than grade II or III tumors (p = 0.008). (B) Metabolic epicenter location versus tumor histopathological grade for the subgroup of astrocytomas alone. Again, grade IV tumors had a significantly deeper metabolic epicenter location than grade II and III tumors (p = 0.047).*

coordinates of the max Cho voxel. Normalized coordinates were used for this calculation and generated by dividing the coordinate values for each patient by the maximum observed coordinate values in the patient cohort. Mean distances were computed for each histopathological grade and compared using one-way analysis of variance (ANOVA). Posthoc tests included the Bonferroni's multiple comparisons test for between-group comparisons and the post-test for linear trend. Finally, the relationship between grade and metabolic epicenter location was evaluated using multinomial logistic regression analysis. Again, age and KPS were controlled for in each model. Statistical analysis was performed using the NCSS statistical software package (NCSS Software: Kaysville, Utah, USA).

Ethics Approval

This study was approved by the Ethics Committee of the Montreal Neurological Institute and Hospital.

Results

Patient Survival and Tumor Histopathological Grade

Patients survived for a median length of 26.8 months (range 0.2-110.9 months) after ^{1}H-MRSI examination. Based on histopathological analysis, 35% (n = 19) of the tumors were WHO grade II, 26% (n = 14) were grade III, and 39% (n = 21) were grade IV (Table 1). For the subgroup of astrocytomas, median survival was 11.7 months (range 0.2 - 108.7 months), with 24% (n = 9) grade II, 19% (n = 7) grade III and 57% (n = 21) grade IV.

Metabolic Epicenter Location: Raw Data

Raw X, Y, and Z coordinates of the max Cho voxel are reported for each patient in Table 1.

Metabolic Epicenter Location and Survival

The results of Cox proportional hazards regression analysis are summarized in Table 2. In correlating metabolic epicenter location to survival, the best regression model included as features the X coordinate, the Z coordinate, and the product of the X and Z coordinates, also known as the XZ interaction term. The Y coordinate was not significant in this model. The model fit the survival data significantly better than chance ($\chi^2 = 19.6$, df = 3, p = 0.0002) and was able to account for 30% of the variability in patient survival ($r^2 = 0.30$). The best model based on histopathological grade alone also fit the data better than chance ($\chi^2 = 47.4$, df = 2, $p < 0.0001$) and accounted for 58% of the variability in survival ($r^2 = 0.58$). When grade and metabolic epicenter location were both included as prognostic factors, the best resulting model showed that grade, X coordinate, Z coordinate, and the XZ interaction term all remained significant predictors of survival ($p < 0.02$), suggesting that metabolic epicenter location and grade are prognostically independent. This combined model fit the survival data best ($\chi^2 = 69$, df = 7, $p < 0.0001$) and accounted for 70% of variability in survival ($r^2 = 0.70$). In a subgroup evaluation of only astrocytomas, it was noted that the best model based on distance of the metabolic epicenter alone was able to account for 32% of the variability in patient survival ($r^2 = 0.32$, p = 0.017), while the best model based on histopathological grade alone accounted for 69% of the variability in survival ($r^2 = 0.69$, p = 0.001). When all features, including grade and metabolic epicenter location were included, the best model accounted for 73% of the variability, ($r^2 = 0.73$, p = 0.001), but the X coordinate, Z coordinate and distance to metabolic epicenter were no longer significantly additive as predictors of survival, although there was a trend towards significance, and this was likely the result of a smaller sample size.

https://doi.org/10.1017/S0317167100008301 Published online by Cambridge University Press

Table 3: Results of multinomial logistic regression modeling: significance and regression coefficients of features between spectroscopic tumor location and histopathological grade

Feature[a]	χ^2 [b]	df[c]	B [SE] [d]	p-value*
Complete model [r^2 =0.25]	27.5	6		0.0001
Z coordinate	15	2	II: 0.2 [0.09] III: 0.2 [0.09]	0.0005
X coordinate	15	2	II: 25 [9] III: 28 [10]	0.0005
X* Z	10	2	II: -0.7 [0.4] III: -1 [0.4]	0.008

[a]Feature = individual factors contained in the regression model. Strength of correlation is indicated by r^2; [b]χ^2= Chi-squared ratio; [c]df = degrees of freedom; [d]B = regression coefficient; SE = standard error
*only features attaining statistical significance at a level of $p < 0.05$ are included here.

Metabolic Epicenter Location and Tumor Histopathological Grade

The mean normalized distance of the metabolic epicenter from the zero point was 0.90 ± 0.055 for grade II, 0.85 ± 0.051 for grade III, and 0.67 ± 0.0056 for grade IV tumors (Figure 2). One-way ANOVA showed the means to be statistically different from each other ($p = 0.008$). Based on Bonferroni's multiple comparisons post-hoc test, grade IV tumors on average had a metabolic epicenter located closer to the zero point than grade III ($p < 0.05$) or grade II ($p < 0.01$) tumors. The post-test for linear trends confirmed that increasing grade correlated with increasingly deeper metabolic epicenter location ($p = 0.003$). For the subgroup of astrocytomas, the mean normalized distance of the metabolic epicenter from the zero point was 0.90 ± 0.058 for grade II, 0.88 ± 0.090 for grade III and 0.69 ± 0.058. One way ANOVA showed the means to be statistically different from each other ($p = 0.047$) but post-hoc tests failed to show further significant trends, likely due to the smaller group sizes. When grade II and III tumors were combined, it was noted that they had a metabolic epicenter further from the zero point than grade IV tumors ($p = 0.013$).

The results of multinomial logistic regression modeling relating tumor grade to metabolic epicenter location are summarized in Table 3. The X coordinate, Z coordinate, and XZ interaction term were all significantly related to tumor grade, independently ($\chi^2 > 10$, df = 2, $p \leq 0.008$ in all cases) and taken together ($\chi^2 = 27.5$, df = 6, $p = 0.0001$). The higher grade tumors had a metabolic epicenter location closer to the zero point than their lower grade counterparts (Figure 3). When the analysis was repeated for the astrocytoma subgroup alone, the X coordinate and mean normalized distance remained significantly related to tumor grade ($\chi^2 = 4.8$, df = 2, $p = 0.029$ and $\chi^2 = 6.5$, df = 2, $p = 0.011$, respectively), but the other interactions terms were no longer significantly related. This likely reflects the small sample size, especially fewer grade III tumors in the astrocytoma subgroup.

Discussion

The results of this study suggest that the location of metabolic epicenter, as defined by the position of the intratumoral voxel containing max Cho on *in vivo* ^{1}H-MRSI, is significantly related to length of survival independent of tumor grade. This finding held true for our combined population of glial tumors, and also for a subgroup evaluating only the astrocytomas. To our

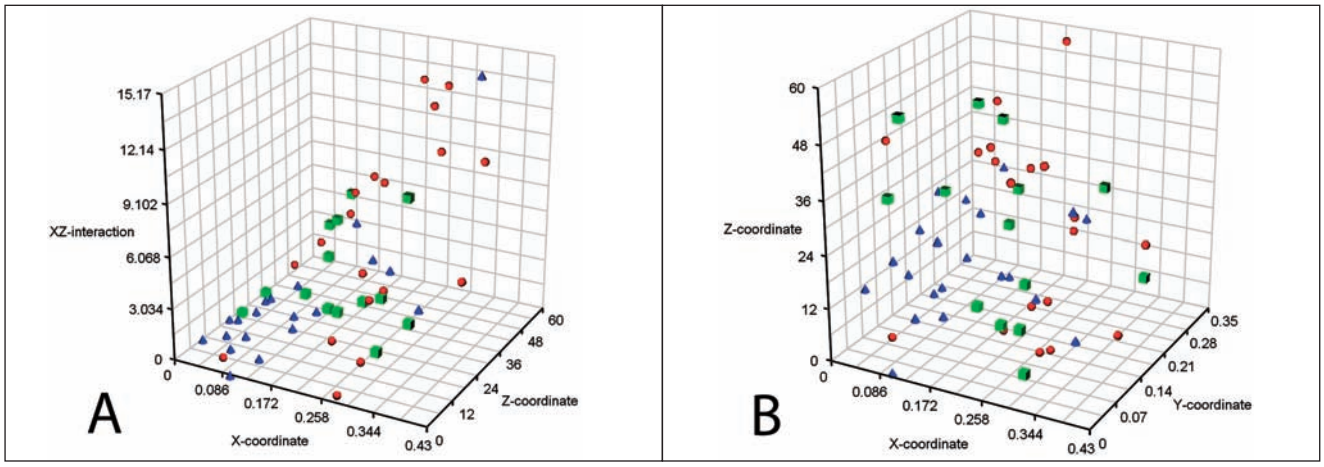

Figure 3: Three-dimensional scatterplots of metabolic epicenter location. Each point represents the position of the metabolic epicenter for a given patient. The origin of each scatterplot is the midpoint of the supratentorial space. Tumors are grouped by WHO grade: red circles = grade II, green squares = grade III, blue triangles = grade IV. (A) Tumor location within the XZ plane alone. (B) Metabolic epicenter location in the X, Y, and Z planes. High-grade tumors converge to the midpoint. On both plots, the positions of metabolic epicenters of low-grade tumors are more scattered than those of the higher grade tumors.

https://doi.org/10.1017/S0317167100008301 Published online by Cambridge University Press

knowledge, this study is also the first to show a significant relationship between glioma location and histopathological grade, when location is defined by a quantitative, easy to measure surrogate, the metabolic epicenter.

Advantages of Using a Metabolic Definition of Glioma Location

Studies addressing glioma location have usually done so in the context of large multivariate analyses of various prognostic factors and the effects of these factors on outcome.[6,11,13,31-44] In addition, two recent epidemiological studies from Finland[45] and France[46] have examined the incidence of gliomas by location. In most of these studies, tumors are typically classified by their position in the frontal, parietal, temporal, or occipital lobes.[6,13,31-39,45] Other studies distinguish between tumors that are lobar or nonlobar,[11] superficial or deep,[40-42] or situated in eloquent versus non-eloquent areas.[46] Devaux et al[43] classified gliomas according to cortical, subcortical, midline, or brainstem locations, while Shinoda et al[44] subdivided location into three subgroups based on the eloquence of the brain underlying the tumor.

Most of these studies found no correlation between glioma location and length of survival,[6,33,34,39,43,44] or did not look for the presence of such a correlation.[45,46] Coffey et al,[11] however, reported that lobar gliomas overall tended to have a better prognosis than nonlobar gliomas. Gehan and Walker[37] found that parietal lobe tumors were associated with shorter survival times than lesions located elsewhere. Among malignant gliomas (i.e., WHO grade II or higher), frontal lobe location also appears to be associated with prolonged survival: Jeremic et al in three separate studies,[13,33,34] Simpson et al,[35] and Curran et al[36] found that frontal lobe location independently predicted increased survival times in patients with tumors classified as WHO grade III or higher. Superficial location also may portend a more favorable prognosis, both for GBMs as reported by Jelsma and Bucy,[40,41] and for malignant gliomas as a whole, as reported by Winger et al.[42]

That previous findings on the nature of relationships between brain tumor location and prognosis are conflicting is expected. First, relatively few studies have examined the issue systematically. Furthermore, the lack of a standard descriptive classification system for tumor location makes it difficult to compare individual studies. In this study we used metabolic information, obtained in an automated fashion via ^{1}H-MRSI, to define tumor location as a single point in space called the metabolic epicenter. This approach removes the possibility of misclassifying, for example, tumors whose margins may be ill-defined or that straddle the boundaries between different cerebral lobes. Furthermore, it uses a standardized stereotactic coordinate system, allowing tumor location data to be compared between patients with varying head and brain sizes. Finally, by accounting for the characteristic regional biological and behavioural heterogeneity of gliomas, the approach is able to account for the fact that tumors appearing to arise from the same part of the brain may in fact have different centers of metabolic activity, which may in turn produce differences in their overall growth and impact on survival.

Relationship between Metabolic Epicenter Location and Survival

Our results showed that a superficial metabolic epicenter location was significantly related to increased survival. In contrast, as the metabolic epicenter converged to the midpoint of the brain, length of survival shortened.

Previous studies reporting increased survival times with more superficially located tumors have speculated that such lesions are more surgically accessible and hence more readily resected.[40,41,47] There is also mounting evidence that more extensive surgical resection is associated with longer life expectancy in patients with glioma, irrespective of grade. In our study, the location of the metabolic epicenter on pre-operative imaging studies predicted survival independently of other patient factors or tumor grade.[48] This held true in both the combined population of tumors, and in the subgroup comprised only of astrocytomas, and was a robust predictor of survival on its own but also improved the model when combined with other features, strongly supporting the notion that the location of the metabolic epicenter is related to genuine biological and biophysical characteristics of gliomas in the supratentorial compartment. One of the weaknesses of our study is that surgical debulking could not be evaluated because we did not consistently have MRI data from the immediate postoperative period from which residual tumor volume could be calculated. Future studies incorporating objective, volumetric data on the extent of surgical resection in combination with ^{1}H-MRSI assessment of the metabolic epicenter are needed to determine if surgery has a greater effect on the magnitude of the relationship between metabolic location and survival than we have predicted.

Relationship between Metabolic Epicenter Location and Histopathological Grade

Our finding of a significant relationship between metabolic epicenter location and histopathological grade, implying that the most metabolically active portion of high-grade tumors converges to the midpoint of the brain, is novel and interesting. This finding follows logically from existing studies on glioma expansion and invasion. It is widely accepted that, unlike other brain neoplasms, both benign and malignant gliomas infiltrate surrounding brain parenchyma by contiguous spread from a very early stage in their development.[14] The mechanisms responsible for glioma invasion at the molecular and cellular levels are still a source of intense investigation, but nonetheless patterns common to gross invasion have been observed. Chief among these is that gliomas spread predominantly through white matter tracts, first postulated more than a century ago by Strobe (as cited by Mikkelsen et al)[14] and later detailed during the first half of the 20th century by Scherer.[49]

The spread of malignant gliomas through most large white matter tracts, including the corpus callosum, uncinate fasciculus, fasciculus longitudinalis, fasciculus occipitofrontalis, auditory and visual bundles, and the corona radiata, has been documented both pathologically[50] and using conventional MRI.[51,52] GBMs in particular tend to invade deep supratentorial structures by expanding vertically in the white matter. As many as 20% of GBMs show such invasion at autopsy.[53] Our finding that the highest grade tumors had their metabolic epicenters in the deep

https://doi.org/10.1017/S0317167100008301 Published online by Cambridge University Press

white matter closest to the midpoint of the supratentorial space is consistent with these prior observations. It further suggests that supratentorial GBMs may be more likely to originate and expand from foci within the deep white matter of the cerebral hemispheres.

Malignant degeneration or dedifferentiation leading to recurrence at a higher histopathological grade is a well-described phenomenon in low-grade gliomas. Its incidence is estimated at 13 to 86%.[54-60] Our data suggest that the acquisition of increasing histological malignancy, detected microscopically, may be accompanied by a stereotyped, macroscopic glioma growth pattern in the supratentorial compartment. Conceivably, as a low-grade tumor dedifferentiates, it may invade in a preferentially deeper direction. The result would be a high-grade tumor with its metabolic epicenter positioned closer to the cerebral zero point. A more interesting explanation is that even if growth by a low-grade glioma occurs equally in all directions, tumor cells may have a tendency to become malignant only when they reach deeper locations in the cerebral hemispheres. This would imply that location may be a determinant of histology, a hypothesis that has previously been suggested,[46] and for which evidence is mounting as investigators examine deep locations—such as the subventricular zone—thought to contain neural stem cells which may give rise to GBM.[61] The preponderantly deep metabolic epicenters of grade IV tumors that we observed might be explained by the existence of a biochemical milieu in these deep locations favouring the development of GBMs, whether arising de novo or secondarily.

Preliminary serial ^{1}H-MRSI assessments in selected patients at our center do in fact suggest that the metabolic epicenter of a tumor migrates toward the cerebral zero point as it develops increasingly malignant histology (Figure 4). This phenomenon may eventually have implications in predicting patterns of glioma recurrence and in designing appropriate targeting strategies for radiotherapy. In particular, it suggests that attacking large superficial portions of a glioma with surgery or radiation may not be of benefit if the deep metabolic epicenter is left intact. Of course this prediction needs to be confirmed in rigorous prospective studies tracking the location of the metabolic epicenter over time in individual patients. In addition, it will be important to study the relationship of metabolic epicenter to behaviour across other tumor types.

We have demonstrated a novel method of assessing supratentorial glioma location by defining the so-called metabolic epicenter in a series of patients as the coordinate position of the voxel containing maximum intratumoral Cho on ^{1}H-MRSI scanning. The concept of the metabolic epicenter eliminates several of the problems related to existing methods of classifying glioma location. Furthermore, our finding that the location of the metabolic epicenter is strongly correlated with overall survival and histopathological grade, suggests that it is reflective of biological factors which influence glioma genesis, expansion, and malignant dedifferentiation. Our findings point to clinical implications in predicting patterns of local tumor recurrence, and in planning resective surgery and radiotherapy.

Acknowledgments

This study was presented by Dr. Sankar in part at the 2007 Joint Annual Meeting of the International Society for Magnetic Resonance in Medicine—European Society for Magnetic Resonance in Medicine and Biology (ISMRM—ESMRMB), May 19-25, 2007, Berlin, Germany. This study was funded in part by the Newsome Endowed Chair in Neurosurgery Research held by Dr. Preul at the Barrow Neurological Institute.

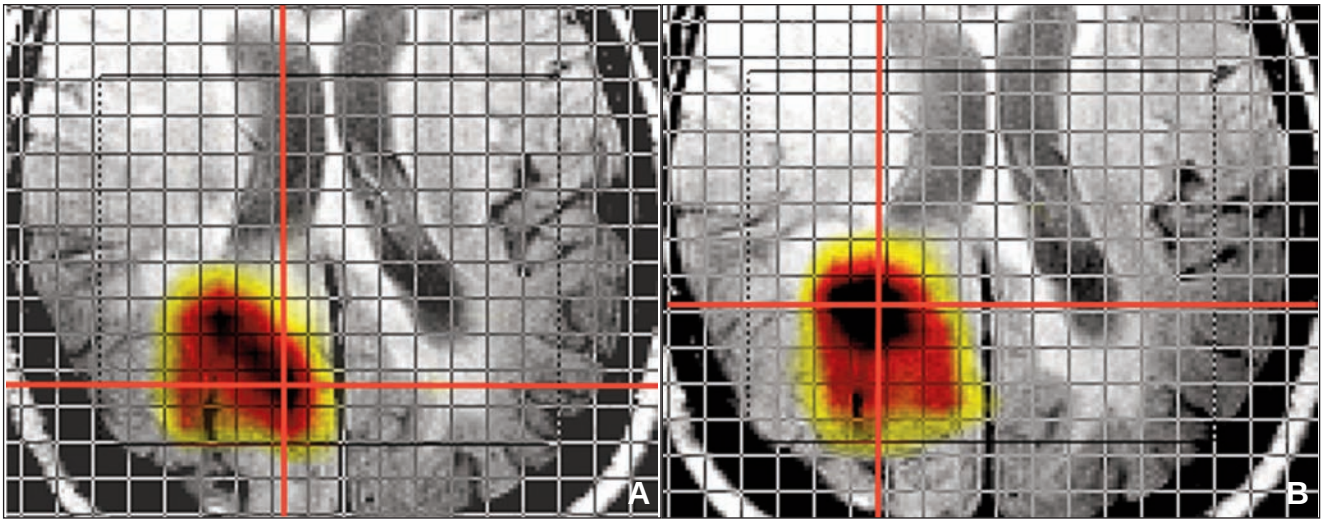

Figure 4: *Intratumoral Cho metabolite map, on a single axial ^{1}H-MRSI slice, of a low-grade supratentorial glioma in a single patient (A) before malignant dedifferentiation and (B) after transformation to a biopsy-confirmed GBM. Crosshairs indicate the position of the metabolic epicenter. Worsening tumor grade is associated with migration of the metabolic epicenter toward the cerebral zero point.*

https://doi.org/10.1017/S0317167100008301 Published online by Cambridge University Press

References

1. Apuzzo MLJ. Commentary: epidemiology and data analysis. In: Apuzzo MLJ, editor. Malignant cerebral glioma. Park Ridge, Ill: American Association of Neurological Surgeons; 1990. p. 111.
2. Ahlbom A, Rodvall Y. Brain tumour trends. Lancet. 1989;334: 1272-3.
3. Salcman M. Epidemiology and factors affecting survival. In: Apuzzo MLJ, editor. Malignant cerebral glioma. Park Ridge, Ill: American Association of Neurological Surgeons; 1990. p. 95-109.
4. Cohadon F, Aouad N, Rougier A, Vital C, Rivel J, Dartigues JF. Histologic and non-histologic factors correlated with survival time in supratentorial astrocytic tumors. J Neurooncol. 1985;3: 105-11.
5. Curran WJ, Jr., Scott CB, Horton J, Nelson JS, Weinstein AS, Fischbach AJ, et al. Recursive partitioning analysis of prognostic factors in three Radiation Therapy Oncology Group malignant glioma trials. J Natl Cancer Inst. 1993;85:704-10.
6. Miller PJ, Hassanein RS, Giri PG, Kimler BF, O'Boynick P, Evans RG. Univariate and multivariate statistical analysis of high-grade gliomas: the relationship of radiation dose and other prognostic factors. Int J Radiat Oncol Biol Phys. 1990;19:275-80.
7. Kim TS, Halliday AL, Hedley-Whyte ET, Convery K. Correlates of survival and the Daumas-Duport grading system for astrocytomas. J Neurosurg. 1991;74:27-37.
8. Chang CH, Horton J, Schoenfeld D, Salazer O, Perez-Tamayo R, Kramer S, et al. Comparison of postoperative radiotherapy and combined postoperative radiotherapy and chemotherapy in the multidisciplinary management of malignant gliomas. A joint Radiation Therapy Oncology Group and Eastern Cooperative Oncology Group study. Cancer. 1983;52:997-1007.
9. Green SB, Byar DP, Walker MD, Pistenmaa DA, Alexander E Jr, Batzdorf U, et al. Comparisons of carmustine, procarbazine, and high-dose methylprednisolone as additions to surgery and radiotherapy for the treatment of malignant glioma. Cancer Treat Rep. 1983;67:121-32.
10. Kinsella TJ, Collins J, Rowland J, Klecker Jr R, Wright D, Katz D, et al. Pharmacology and phase I/II study of continuous intravenous infusions of iododeoxyuridine and hyperfractionated radiotherapy in patients with glioblastoma multiforme. J Clin Oncol. 1988;6:871-9.
11. Coffey RJ, Lunsford LD, Taylor FH. Survival after stereotactic biopsy of malignant gliomas. Neurosurgery. 1988;22:465-73.
12. Nelson DF, Nelson JS, Davis DR, Chang CH, Griffin TW, Pajak TF. Survival and prognosis of patients with astrocytoma with atypical or anaplastic features. J Neurooncol. 1985;3:99-103.
13. Jeremic B, Milicic B, Grujicic D, Dagovic A, Aleksandrovic J, Nikolic N. Clinical prognostic factors in patients with malignant glioma treated with combined modality approach. Am J Clin Oncol. 2004;27:195-204.
14. Mikkelsen T, Enam SA, Rosenblum ML. Invasion in malignant glioma. In: Winn HR, Youmans JR, editors. Youmans Neurological Surgery. Philadelphia: Saunders; 2004. p. 757-70.
15. Preul MC, Caramanos Z, Collins DL, Villemure JG, Leblanc R, Olivier A, et al. Accurate, noninvasive diagnosis of human brain tumors by using proton magnetic resonance spectroscopy. Nat Med. 1996;2:323-5.
16. Preul MC, Caramanos Z, Leblanc R, Villemure JG, Arnold DL. Using pattern analysis of in vivo proton MRSI data to improve the diagnosis and surgical management of patients with brain tumors. NMR Biomed. 1998;11:192-200.
17. McBride DQ, Miller BL, Nikas DL, Buchthal S, Chang L, Chiang F, et al. Analysis of brain tumors using 1H magnetic resonance spectroscopy. Surg Neurol. 1995;44:137-44.
18. Meyerand ME, Pipas JM, Mamourian A, Tosteson TD, Dunn JF. Classification of biopsy-confirmed brain tumors using single-voxel MR spectroscopy. AJNR Am J Neuroradiol. 1999;20: 117-23.
19. Castillo M, Kwock L, Scatliff J, Mukherji SK. Proton MR spectroscopy in neoplastic and non-neoplastic brain disorders. Magn Reson Imaging Clin N Am. 1998;6:1-20.
20. Alger JR, Frank JA, Bizzi A, Fulham MJ, DeSouza BX, Duhaney MO, et al. Metabolism of human gliomas: assessment with H-1 MR spectroscopy and F-18 fluorodeoxyglucose PET. Radiology. 1990;177:633-41.
21. Fulham MJ, Bizzi A, Dietz MJ, Shih HH, Raman R, Sobering GS, et al. Mapping of brain tumor metabolites with proton MR spectroscopic imaging: clinical relevance. Radiology. 1992;185: 675-86.
22. Fountas KN, Kapsalaki EZ, Gotsis SD, Kapsalakis JZ, Smisson III HF, Johnston KW, et al. In vivo proton magnetic resonance spectroscopy of brain tumors. Stereotact Funct Neurosurg. 2000; 74:83-94.
23. Tamiya T, Kinoshita K, Ono Y, Matsumoto K, Furuta T, Ohmoto T. Proton magnetic resonance spectroscopy reflects cellular proliferative activity in astrocytomas. Neuroradiol. 2000;42: 333-8.
24. Wilken B, Dechent P, Herms J, Maxton C, Markakis E, Hanefeld F, et al. Quantitative proton magnetic resonance spectroscopy of focal brain lesions. Pediatr Neurol. 2000;23:22-31.
25. Shimizu H, Kumabe T, Tominaga T, Kayama T, Hara K, Ono Y, et al. Noninvasive evaluation of malignancy of brain tumors with proton MR spectroscopy. AJNR Am J Neuroradiol. 1996;17: 737-47.
26. Dowling C, Bollen AW, Noworolski SM, McDermott MW, Barbaro NM, Day MR, et al. Preoperative proton MR spectroscopic imaging of brain tumors: correlation with histopathologic analysis of resection specimens. AJNR. 2001;22:604-12.
27. Tedeschi G, Lundbom N, Raman R, Bonavita S, Duyn JH, Alger JR, et al. Increased choline signal coinciding with malignant degeneration of cerebral gliomas: a serial proton magnetic resonance spectroscopy imaging study. J Neurosurg. 1997;87: 516-24.
28. McKnight TR, Lamborn KR, Love TD, Berger MS, Chang S, Dillon WP, et al. Correlation of magnetic resonance spectroscopic and growth characteristics within Grades II and III gliomas. J Neurosurg. 2007;106:660-6.
29. Matsumura A, Isobe T, Anno I, Takano S, Kawamura H. Correlation between choline and MIB-1 index in human gliomas. A quantitative proton MR spectroscopy study. J Clin Neurosci. 2005;12:416-20.
30. Kwan RK, Evans AC, Pike GB. MRI simulation-based evaluation of image-processing and classification methods. IEEE Trans Med Imaging. 1999;18:1085-97.
31. Jeremic B, Grujicic D, Antunovic V, Djuric L, Stojanovic M, Shibamoto Y. Hyperfractionated radiation therapy (HFX RT) followed by multiagent chemotherapy (CHT) in patients with malignant glioma: a phase II study. Int J Radiat Oncol Biol Phys. 1994;30:1179-85.
32. Jeremic B, Grujicic D, Antunovic V, Djuric L, Shibamoto Y. Accelerated hyperfractionated radiation therapy for malignant glioma. A phase II study. Am J Clin Oncol. 1995;18:449-53.
33. Jeremic B, Shibamoto Y, Grujicic D, Milicic B, Stojanovic M, Nikolic N, et al. Pre-irradiation carboplatin and etoposide and accelerated hyperfractionated radiation therapy in patients with high-grade astrocytomas: a phase II study. Radiother Oncol. 1999;51:27-33.
34. Jeremic B, Shibamoto Y, Grujicic D, Stojanovic M, Milicic B, Nikolic N, et al. Concurrent accelerated hyperfractionated radiation therapy and carboplatin/etoposide in patients with malignant glioma: long-term results of a phase II study. J Neurooncol. 2001;51:133-41.
35. Simpson JR, Horton J, Scott C, Curran WJ, Rubin P, Fischbach J, et al. Influence of location and extent of surgical resection on survival of patients with glioblastoma multiforme: results of three consecutive Radiation Therapy Oncology Group (RTOG) clinical trials. Int J Radiat Oncol Biol Phys. 1993;26:239-44.
36. Curran WJ, Jr., Scott CB, Horton J, Nelson JS, Weinstein AS, Nelson DF. Does extent of surgery influence outcome for astrocytoma with atypical or anaplastic foci (AAF)? A report from three Radiation Therapy Oncology Group (RTOG) trials. J Neurooncol. 1992;12:219-27.
37. Gehan EA, Walker MD. Prognostic factors for patients with brain tumors. Natl Cancer Inst Monogr. 1977;46:189-95.

38. Phuphanich S, Ferrall S, Greenberg H. Long-term survival in malignant glioma. Prognostic factors. J Fla Med Assoc. 1993;80:181-4.
39. Kowalczuk A, Macdonald RL, Amidei C, Dohrmann III G, Erickson RK, Hekmatpanah J, et al. Quantitative imaging study of extent of surgical resection and prognosis of malignant astrocytomas. Neurosurgery. 1997;41:1028-36.
40. Jelsma R, Bucy PC. Glioblastoma multiforme: its treatment and some factors affecting survival. Arch Neurol. 1969;20:161-71.
41. Jelsma R, Bucy PC. The treatment of glioblastoma multiforme of the brain. J Neurosurg. 1967;27:388-400.
42. Winger MJ, Macdonald DR, Cairncross JG. Supratentorial anaplastic gliomas in adults. The prognostic importance of extent of resection and prior low-grade glioma. J Neurosurg. 1989;71:487-93.
43. Devaux BC, O'Fallon JR, Kelly PJ. Resection, biopsy, and survival in malignant glial neoplasms. A retrospective study of clinical parameters, therapy, and outcome. J Neurosurg. 1993;78: 767-75.
44. Shinoda J, Sakai N, Murase S, Yano H, Matsuhisa T, Funakoshi T. Selection of eligible patients with supratentorial glioblastoma multiforme for gross total resection. J Neurooncol. 2001;52: 161-71.
45. Larjavaara S, Mantyla R, Salminen T, Haapasalo H, Raitanen J, Jaaskelainen J, et al. Incidence of gliomas by anatomic location. Neuro Oncol. 2007;9:319-25.
46. Duffau H, Capelle L. Preferential brain locations of low-grade gliomas: comparison with glioblastomas and review of hypothesis. Cancer. 2004;100:2622-6.
47. Walker MD, Green SB, Byar DP, Alexander E Jr, Batzdorf U, Brooks WH, et al. Randomized comparisons of radiotherapy and nitrosoureas for the treatment of malignant glioma after surgery. N Engl J Med. 1980;303:1323-9.
48. Sanai N, Berger MS. Glioma extent of resection and its impact on patient outcome. Neurosurgery. 2008;62:753-66.
49. Scherer HJ. Structural development in gliomas. Am J Cancer. 1938; 34:333-51.
50. Matsukado Y, MacCarty CS, Kernohan JW. The growth of glioblastoma multiforme (astrocytomas, grades 3 and 4) in neurosurgical practice. J Neurosurg. 1961;18:636-44.
51. Rosenblum ML, Eisenberg AD, Norman D. Brain tumor invasion: clinical patterns of malignant astrocytoma spread [abstract]. J Neurosurg. 1992;76:383A.
52. Enam SA, Eisenberg AD, Norman D, Rosenblum ML. Patterns of spread and recurrence of glioma: studies by neuroimaging. In: Mikkelsen T, Bjerkvig R, Laerum OD, Rosenblum ML, editors. Brain tumor invasion: biological, clinical, and therapeutic considerations. New York: Wiley-Liss; 1998. p. 133-59.
53. Salazar OM, Rubin P. The spread of glioblastoma multiforme as a determining factor in the radiation treated volume. Int J Radiat Oncol Biol Phys. 1976;1:627-37.
54. Piepmeier JM. Observations on the current treatment of low-grade astrocytic tumors of the cerebral hemispheres. J Neurosurg. 1987;67:177-81.
55. McCormack BM, Miller DC, Budzilovich GN, Voorhees GJ, Ransohoff J. Treatment and survival of low-grade astrocytoma in adults—1977-1988. Neurosurgery. 1992;31:636-42.
56. Laws ER, Jr., Taylor WF, Clifton MB, Okazaki H. Neurosurgical management of low-grade astrocytoma of the cerebral hemispheres. J Neurosurg. 1984;61:665-73.
57. Muller W, Afra D, Schroder R. Supratentorial recurrences of gliomas. Morphological studies in relation to time intervals with astrocytomas. Acta Neurochir (Wien). 1977;37:75-91.
58. North CA, North RB, Epstein JA, Piantadosi S, Wharam MD. Low-grade cerebral astrocytomas. Survival and quality of life after radiation therapy. Cancer. 1990;66:6-14.
59. Soffietti R, Chio A, Giordana MT, Vasario E, Schiffer D. Prognostic factors in well-differentiated cerebral astrocytomas in the adult. Neurosurgery. 1989;24:686-92.
60. Vertosick FT Jr, Selker RG, Arena VC. Survival of patients with well-differentiated astrocytomas diagnosed in the era of computed tomography. Neurosurgery. 1991;28:496-501.
61. Lim DA, Cha S, Mayo MC, Chen M-H, Keles E, VandenBerg S, et al. Relationship of glioblastoma multiforme to neural stem cell regions predicts invasive and multifocal tumor phenotype. Neurooncol. 2007;9:424-9.